Heliyon 10 (2024) e34203

Contents lists available at ScienceDirect

Heliyon

journal homepage: www.cell.com/heliyon

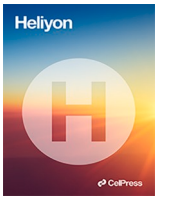

Research article

Exosomal lncRNA HCP5 derived from human bone marrow mesenchymal stem cells improves chronic periodontitis by miR-24-3p/*HO1/P38/ELK1* pathway

Yu Liu [a,1], Jin Zhu [a,1], Wei-hong Wang [a], Lian Zeng [b], Yan-ling Yang [b], Zhou Wang [b], Jian-qi Liu [b], Wei Li [b], Jing-yu Sun [b], Xiao-hong Yu [b,*]

[a] *Department of Oral and Maxillofacial Surgery, Affiliated Stomatology Hospital of Kunming Medical University, Kunming 650106, Yunnan, China*
[b] *Department of Oral Medicine, the Affiliated Hospital of Yunnan University (Second People's Hospital of Yunnan Province, Yunnan Province Ophthalmology Hospital), Kunming 650031, Yunnan, China*

A R T I C L E I N F O

Keywords:
Human bone marrow mesenchymal stem cells
Exosomes
lncRNA HCP5
Human periodontal ligament stem cells
Osteogenic differentiation
miR-24-3p

A B S T R A C T

Objective: The present study aimed to explore the function of human bone marrow mesenchymal stem cells (hBMMSCs)-derived exosomal long noncoding RNA histocompatibility leukocyte antigen complex P5 (HCP5) in the osteogenic differentiation of human periodontal ligament stem cells (hPDLSCs) to improve chronic periodontitis (CP).

Methods: Exosomes were extracted from hBMMSCs. Alizarin red S staining was used to detect mineralised nodules. Reverse transcription-quantitative polymerase chain reaction (RT-qPCR) was used to measure HCP5 and miR-24-3p expression. The mRNA and protein levels of alkaline phosphatase (*ALP*), osteocalcin, osterix, runt-related transcription factor 2, bone morphogenetic protein 2, osteopontin, fibronectin, collagen 1, heme oxygenase 1 (*HO1*), *P38*, and ETS transcription factor ELK1 (*ELK1)* were detected using RT-qPCR and Western blot. Enzyme-linked immunosorbent assay (ELISA) kits were used to determine the HO1 and carbon monoxide concentrations. Heme, biliverdin, and Fe^{2+} levels were determined using detection kits. Microcomputed tomography, hematoxylin and eosin staining, ALP staining, tartrate-resistant acid phosphatase staining, ELISA, and RT-qPCR were conducted to evaluate the effect of HCP5 on CP mice. Dual luciferase, RNA immunoprecipitation, and RNA pulldown experiments were performed to identify the interactions among HCP5, miR-24-3p, and *HO1*.

Results: The osteogenic ability of hPDLSCs significantly increased when co-cultured with hBMMSCs or hBMMSCs exosomes. Overexpression of HCP5 and *HO1* in hBMMSCs exosomes promoted the osteogenic differentiation of hPDLSCs, and knockdown of HCP5 repressed the osteogenic differentiation of hPDLSCs. HCP5 knockdown enhanced the inflammatory response and repressed osteogenesis in CP mice. MiR-24-3p overexpression diminished the stimulatory effect of HCP5 on the osteogenic ability of hPDLSCs. Mechanistically, HCP5 acted as a sponge for miR-24-3p and regulated *HO1* expression, and *HO1* activated the *P38/ELK1* pathway.

Conclusion: HBMMSCs-derived exosomal HCP5 promotes the osteogenic differentiation of hPDLSCs and alleviates CP by regulating the miR-24-3p/*HO1/P38/ELK1* signalling pathway.

* Corresponding author. Department of Oral Medicine, Affiliated Hospital of Yunnan University (Second People's Hospital of Yunnan Province, Yunnan Province Ophthalmology Hospital), Kunming 650031, QingNian road 176, Yunnan, China.
E-mail address: joyyao100@hotmail.com (X.-h. Yu).
[1] Yu Liu and Jin Zhu contributed equally to this work.

https://doi.org/10.1016/j.heliyon.2024.e34203
Received 2 July 2023; Received in revised form 26 June 2024; Accepted 4 July 2024
Available online 8 July 2024

1. Introduction

Chronic periodontitis (CP) is a chronic inflammation caused by bacterial infections, such as *Actinobacillus actinomycetemcomitans*, *Porphyromonas gingivalis*, and *Bacteroides repens*. Pathological manifestations include gingival haemorrhage, gingival atrophy, inflammation of the periodontal tissues, formation of periodontal pockets, and alveolar bone resorption. CP often causes loose teeth, shifts or falls off, decreases bite force, and affects patients' normal diet and physical health. In severe cases, it may increase the risk of coronary heart disease, stroke, and diabetes [1]. Ultrasonic scaling is commonly used clinically to remove dental calculus and plaque, and anti-inflammatory drugs are primarily used for treatment. Surgery is required in severe cases; however, the probability of recurrence is high after treatment [2]. Therefore, identifying therapeutic targets for CP is the key to exploring new therapeutic regimens.

Human periodontal ligament stem cells (hPDLSCs) in the periodontal ligament have strong self-renewal and multidirectional differentiation abilities. The osteogenic differentiation of hPDLSCs is the biological basis for alveolar bone regeneration and repair. The induction of osteogenic differentiation of hPDLSCs is important for treating of periodontitis. Exosomes are extracellular vesicles derived from various cells. They carry biological molecules (such as nucleic acids, proteins, and lipids) to transmit signals, mediate intercellular communication, and regulate the biological processes of target cells. Studies have revealed that the exosomes of human bone marrow mesenchymal stem cells (hBMMSCs) are involved in regulating cell osteogenic differentiation [3,4]. However, there is limited research on regulating the osteogenic differentiation of hPDLSCs through hBMMSCs exosomes.

Long noncoding RNAs (lncRNAs) are important regulators of biological processes that regulate the expression of target genes by interacting with RNA, proteins, or DNA to exert biological functions. LncRNAs are closely related to disease recurrence, metastasis, and prognosis. Increasing evidence indicates that exosome-derived lncRNAs are involved in regulating disease development [5,6]. For instance, Behera et al. [5] demonstrated that BMMSCs-derived lncRNA H19 promoted endothelial angiogenesis and osteogenesis by sponging miR-106 and regulating *Angpt1*. The lncRNA histocompatibility leukocyte antigen complex P5 (HCP5) is a regulator of multiple diseases, including gastric cancer [7], neuroblastoma [8], and allergic rhinitis [9]. HBMMSCs-derived exosomal HCP5 increases the viability of cardiomyocytes following hypoxia/reperfusion and decreases apoptosis [10]. HCP5 inhibits high glucose-induced inflammation in human glomerular mesangial cells [11]. HCP5 expression decreases in allergic rhinitis and promotes the differentiation of regulatory T-cell [9]. In competitive endogenous RNA mechanisms, lncRNAs regulate mRNA expression through sponging miRNAs. The competitive endogenous RNA mechanism provides a new avenue for identifying disease therapeutic targets and has become a hot research topic. Liu et al. [12] showed that HCP5, as a sponge of miR-128-3p, promoted the growth of multiple myeloma by promoting PLAG1 like zinc finger 2 expression and activating the Wnt/β-catenin/cyclin D1 signalling pathway. However, the function of HCP5 in CP is unclear.

In this study, we explored the effect of HCP5 on CP by regulating the osteogenic differentiation of hPDLSCs. We found that hBMMSCs-derived exosomal HCP5, acting as a sponge for miR-24-3p, promoted osteogenic differentiation by upregulating heme oxygenase 1 (*HO1*) and activating the *P38*/ETS transcription factor (*ELK1*) signalling pathway. Knockdown of hBMMSCs-derived exosomal HCP5 increases the concentration of inflammatory cytokines and suppresses osteogenesis in CP mice. These results indicate that HCP5 is a promising target for treating CP.

2. Materials and methods

2.1. Cell culture

HBMMSCs (catalogue number: HUXMA-01001) were obtained from Cyagen (Guangzhou, China) Biosciences Inc. The hPDLSCs (catalogue number: *C*P-H234) were purchased from Wuhan Procell Life Science & Technology Co., Ltd. HBMMSCs and hPDLSCs were cultured in Dulbecco's modified eagle medium (Wuhan Procell) supplemented with 10 % fetal bovine serum and 1 % penicillin/streptomycin and incubated at 37 °C in a 5 % CO_2 incubator. Myco-Lumi™ luminescence mycoplasma detection kits (Cat: C0298 M, Beyotime, Shanghai, China) were used to detect mycoplasma during cell culture.

2.2. Co-culture of hBMMSCs and hPDLSCs

HBMMSCs were indirectly co-cultured with hPDLSCs through Millicell® hanging cell culture inserts (Millipore, USA) [13]. HBMMSCs (5×10^5 cells/well) were seeded in the upper compartment (inserts), and hPDLSCs (5×10^5 cells/well) were cultured in 6-well plates in the lower compartment. The cells were cultured in a basic culture medium for 12 h, and the inserts were placed into a 6-well plate to obtain an indirect contact co-culture system. The hPDLSCs medium was replaced with an osteogenic induction medium (Wuhan Procell). After co-culturing for 21 days, hPDLSCs were collected for further analysis.

2.3. Isolation of exosomes and characterisation

HBMMSCs were cultured in Dulbecco's modified eagle medium for three days at 37 °C in a 5 % CO_2 incubator. The cell supernatants were collected and centrifuged at 1000 rpm/min and 16000 rpm/min for 10 and 20 min at 4 °C, respectively. The supernatants were collected and centrifuged at 120000 rpm for 150 min at 4 °C. The supernatants were discarded and the precipitates were re-suspended in phosphate-buffered saline. Exosomes were obtained from hBMMSCs.

Table 1
Primer sequences of target.

Target	Sequences (F: Forward primer. R: Reverse primer. 5′-3′)
ALP (H)	F-GAACCTCATCATCTTCCT
	R-CCAGTTTGTCCTTCTTCT
OCN (H)	F-CAGAGTCCAGCAAAGGTG
	R-AGCCATTGATACAGGTAGC
OSX (H)	F-CCCTTTACAAGCACTAAT
	R-ATCATTAGCATAGCCTGA
RUNX2 (H)	F-ACCATAACCGTCTTCACAA
	R-GAGGTCCATCTACTGTAACTT
BMP2 (H)	F-CATCTGAACTCCACTAATC
	R-TTCATTCTCGTCAAGGTA
OPN (H)	F-AATGATGAGAGCAATGAG
	R-GTCTACAACCAGCATATC
FN (H)	F-GAATATGTAGTGAGTGTCT
	R-AGAGTTGGCAGTAATATC
COL-1 (H)	F-AGAAGAACTGGTACATCA
	R-CATACTCGAACTGGAATC
LINC01535 (H)	F-CGGCTGTTCTTCACTGACCT
	R-GAGGGAAAGTCAAGCGTGGA
H19 (H)	F-CGGACGTGATGATCCCTGAG
	R-GCCCTAAGTGGCCAGACATT
MEG3 (H)	F-AGGGGCACTAGGTAGACAGG
	R-CGGGTCTCTACTCAAGGGGA
TUG1 (H)	F-ACGACTGAGCAAGCACTACC
	R-CTCAGCAATCAGGAGGCACA
MSC-AS1 (H)	F-CGGTAAGCTGCGCCTTTTG
	R-TAGAAGCACCGTCGGTAGGA
TWIST1 (H)	F-GGCCATGACTGCTGAGAAGA
	R-ACTTTGGGGAGGGGAACCT
HCP5 (H)	F-CTGTGTCCCAGGAATGGTCC
	R-TGCAGAGGCCCTACTTCTCT
LINC00707 (H)	F-CCAACAGGGTATCAGAATTCTC
	R-TGCTGACAATAGCCATTAGG
XIST (H)	F-TTACTCTCTCGGGGCTGGAA
	R-AGGGTGTTGGGGGACTAGAA
BCAR4 (H)	F-GATAAAATGCCACACAACCAT
	R-CAGAACTCCATAGCCACCAA
ALP (M)	F-GCCAAATGTGGTGTTGCACT
	R-GGACTAACCTACCACCCCAC
OCN (M)	F-CCGTAGATGCGTTTGTAGGC
	R-CCTTGTGTGTCTTCTCCACAG
OSX (M)	F-TCTGACTGCCTGCCTAGT
	R-GTGGATGCCTGCCTTGTA
RUNX2 (M)	F-GCTTGATGACTCTAAACC
	R-ACACCTACTCTCATACTG
BMP2 (M)	F-CTGGTGAACTCTGTGAAT
	R-CTAGGTACAACATGGAGATT
OPN (M)	F-AACTCTTCCAAGCAATTCC
	R-TCTCCATCGTCATCATCAT
FN (M)	F-ATACGAAGTCAGTGTCTA
	R-ATTCTCCAGAGTAGTGAT
COL-1 (M)	F-AGGTATGCTTGATCTGTAT
	R-CAGTCCAGTTCTTCATTG
HCP5 (M)	GACTCTCCTACTGGTGCTTGGT
	CACTGCCTGGTGAGCCTGTT
miR-24-3p (H)	F-TTTGGCTCAGTTCAGCAG
	R-TTTGGCACTAGCACATT
HO1 (H)	F-GACTGCGTTCCTGCTCAA
	R-CTCTGGTCCTTGGTGTCAT
P38 (H)	F-GTTCAGTTCCTTATCTACCA
	R-GCTCACAGTCTTCATTCA
ELK1 (H)	F-GACCAACATGAATTACGA
	R-AACTTGTAGACGAACTTC
GAPDH (H)	F-TTGCCCTCAACGACCACTTT
	R-TGGTCCAGGGGTCTTACTCC
GAPDH (M)	F-TGGAACTCACCCGTTCACAC
	R-CGGGCCACGCTAATCTCAT
U6 (H)	GCTTCGGCAGCACATATACTAAAAT
	R-CGCTTCACGAATTTGCGTGTCAT

2.4. Transmission electron microscope (TEM)

First, 15 μL of an exosome suspension was placed on the TEM sample-loaded copper mesh. The liquid in the copper mesh was removed after 5 min. Then, 2 % uranyl acetate staining solution (15 μL) was added. One minute later, the copper mesh was baked with an incandescent lamp for 10 min, and a JEM-1400 Plus TEM was used to observe the exosomes.

2.5. Inducing osteogenic differentiation of hPDLSCs

HPDLSCs were digested and prepared into single-cell suspensions, and the cells were inoculated into 6-well plates (2×10^5 cells/well) until the cells were amplified to 80 %. The medium was replaced with an osteogenic induction solution. The cells were collected for further analysis after culturing for 21 days.

2.6. Cell transfection and treatment

According to the manufacturer's instructions, an overexpressed empty plasmid (pcDNA-NC), overexpressed HCP5 plasmid (pcDNA-HCP5), sh-RNA negative control (sh-NC), and knockdown HCP5 plasmid (sh-HCP5) (synthesized by Shanghai Genomeditech) were transfected into hBMMSCs using Lipofectamine 2000. Empty plasmids overexpressing miRNA (NC mimic), overexpressed miR-24-3p plasmid (miR-24-3p mimic), pcDNA-NC, pcDNA-HCP5, and overexpressed HO1 plasmid (pcDNA-HO1) (synthesized by Shanghai Genomeditech) were transfected into hPDLSCs using Lipofectamine 2000. The hPDLSCs transfected with pcDNA-HO1 were treated with 10 μM P38 inhibitor PD169316 (P38 phosphorylation inhibitor, Shanghai, Beyotime) for 24 h [14,15].

2.7. Alizarin red S (ARS) staining

After the induction of osteogenic differentiation, hPDLSCs were fixed with a fixative for 20 min. After rinsing, ARS dye solution (Shanghai Beyotime) was added to stain the cells for 30 min. The cells were observed and photographed under an inverted microscope.

2.8. Reverse transcription-quantitative polymerase chain reaction (RT-qPCR)

The total RNA was extracted from cells and tissues using TRIzol reagent (Thermo Fisher Scientific, USA), and the concentration of RNA was measured using an ultraviolet spectrophotometer. The optical density $(OD)_{260}/OD_{280}$ value was 1.8–2.0. The HyperScript III 1st Strand cDNA Synthesis Kit (Shanghai EnzyArtisan) was used for cDNA synthesis. A TB Green® Premix Ex Taq™ II kit (Wuhan U–Me-Biotech) was used for the PCR reaction. The reaction conditions using a thermal cycler were as follows: 95 °C for 30 s, 95 °C for 5 s and 60 °C for 30 s, which were repeated 40 times. The $2^{-\Delta\Delta Ct}$ method was used to analyse the relative expression of target genes. Table 1 lists all primer sequences of the target genes.

2.9. Western blot

RIPA lysates were used to extract total protein from exosomes and cells, and a bicinchoninic acid kit (Shanghai, Beyotime) was used for protein quantification. Protein samples were subjected to polyacrylamide gel electrophoresis and transferred onto polyvinylidene fluoride membranes. The membranes were incubated in a 5 % skim milk powder for 1 h. Membranes were incubated with the primary

Table 2
Antibody information.

Gene	Antibody	Dilution multiple
ALP	Rabbit monoclonal to anti-ALP (ab307726)	1:1000
OCN	Rabbit monoclonal to anti-OCN (ab133612)	1:1000
OSX	Rabbit monoclonal to anti-OSX (ab209484)	1:1000
RUNX2	Rabbit anti-RUNX2 (bs-1134R)	1:1000
BMP2	Rabbit anti-BMP2 (bs-10696R)	1:1000
OPN	Rabbit anti-OPN (bs-23258R)	1:1000
FN	Rabbit monoclonal to anti-FN (ab268020)	1:1000
COL-1	Rabbit monoclonal to anti-COL-1 (ab270993)	1:1000
GAPDH	Rabbit anti-GAPDH (bs-41373R)	1:1000
Alix	Rabbit monoclonal to anti-ALIX (ab275377)	1:1000
CD9	Rabbit anti-CD9 (bs-2489R)	1:1000
CD63	Rabbit monoclonal to anti-CD63 (ab134045)	1:1000
CD81	Rabbit anti-CD81 (bs-6934R)	1:1000
HO1	Rabbit polyclonal to anti-HO1 (ab13243)	1:2000
P38	Rabbit monoclonal to anti-P38 (ab170099)	1:1000
P–P38	Rabbit monoclonal to p38 (phospho T180) (ab178867)	1:1000
ELK1	Rabbit anti-ELK1 (bs-1398R)	1:300
P-ELK1	Rabbit Anti-Phospho (Ser383) (bs-10154R)	1:300
Goat Anti-Rabbit IgG H&L (HRP)	Goat Anti-Rabbit IgG H&L (HRP) (ab6721)	1:2000

and secondary antibodies (Abcam, UK), and developed using a gel imaging instrument after treatment with the enhanced chemiluminescence reagent. Antibodies' information and dilution multiples are listed in Table 2.

2.10. Animals and establishment of the CP mouse model [16]

Twenty-four 10-week-old C57BL/6 male mice were purchased from Hunan Silaikejingda Experimental Animal co., ltd (SCXK (Xiang) 2019–0004). The mice were raised for four weeks at a temperature of 22–25 °C, a relative humidity of 40%–70 %, and 12 h alternation of day and night. The mice had ad libitum access to food and water. This study was approved by the Laboratory Animal Ethics Committee of Yunnan Labreal Biotechnology Co., Ltd (PZ20211113).

The mice were randomly divided into four groups: sham, CP model, CP + exo-sh-NC, and CP + exo-sh-HCP5. First, 5-0 silk was used to establish the CP mouse model. Mice were anaesthetized with 75 mg/kg pentobarbital and fixed on an operating table to expose the oral cavity. The right maxillary second molar of each mouse was ligated with a 5-0 silk thread, and the ligating silk was embedded as far as possible into the gingival sulcus. The silk was checked every three days to prevent it from falling, and the formation of a periodontal pocket and destruction of the alveolar bone were observed. After modelling for six weeks, CP mice were obtained. hBMMSCs derived exosomes transfected with sh-NC (CP + exo-sh-NC group) and sh-HCP5 (CP + exo-sh-HCP5) were injected into the periodontal tissue of maxillary second molars of CP mouse, exosomes were injected every three days for six weeks. The mice were euthanized by intraperitoneal injection of sodium pentobarbital (150 mg/kg). The maxillary bone of mouse was collected for Micro-computed tomography (Micro-CT) staining, the periodontal tissues of experimental teeth were collected for morphological staining and RT-qPCR assay, and Mice serum was collected to measure the concentration of TNF-α, IL-1β, IL-6, IL-8.

2.11. Micro-CT

The samples were fixed with 4 % paraformaldehyde, rinsed with phosphate-buffered saline, and scanned using high-resolution micro-CT. The Micro-CT Skyscan 1276 system (Bruker, Germany) was used top measure the distance of cementoenamel junction-alveolar bone crest (CEJ-ABC) on the sagittal images of selected teeth at 70 kV, 200 μA, and 6.5 μm pixels. Reconstruction was accomplished using NRecon, and CT Analyser was used to analyse the region of interest.

2.12. Hematoxylin and eosin (HE) staining

The maxillary bones of the mice were decalcified with 10 % EDTA for four weeks. Tissues were dehydrated with ethanol, embedded in paraffin, and sectioned using a microtome. Staining was performed using a HE kit (Shanghai Beyotime) according to the manufacturer's instructions. Sections were dewaxed with xylene, ethanol, and distilled water, stained with hematoxylin for 2 min, rinsed, and stained with eosin for 10 s. Sections were treated with ethanol and xylene, sealed with neutral glue, and observed under a microscope.

2.13. Alkaline phosphatase (ALP) staining

Decalcified tissues were dehydrated in ethanol, soaked overnight in OCT, embedded and sectioned using a freezing microtome. The sections were immersed in distilled water for 60 min, and the water was removed. Sections were incubated with ALP dye solution (Nanjing Jiancheng Bioengineering Institute) for 2 h, followed by incubation with cobalt, sulfuration working solution, and nuclear fast red fixation solution. The sections were rinsed with distilled water, sealed using glycerol, and the results were observed under a microscope.

2.14. Tartrate-resistant acid phosphatase (TRAP) staining

Frozen sections of mouse periodontal tissues were immersed in distilled water for 10 min, and TRAP fixative (Nanjing Jiancheng Bioengineering Institute) was used to fix the sections for 1 min after wiping off the water. After washing and drying the sections, the TRAP reagent was added and incubated at 37 °C for 2 h. Rinsing the sections, methyl green was added dropwise and incubated for 2 s. Sections were sealed with glycerol, followed by microscopic observation.

2.15. Dual luciferase reporter assay

Wild-type (WT) and mutant (MUT) sequences of HCP5 and *HO1* were amplified and inserted into the *p*-mir-Glo vector (Biofeng, China). According to kit instructions, NC mimic, miR-24-3p mimic, and HCP5/*HO1*-WT/MUT were transfected into hPDLSCs using Lipofectamine 2000 (Thermo Fisher Scientific). After 48 h, luciferase activity was detected using a dual luciferase reporter gene detection kit (Promega, China).

2.16. RNA pulldown

An RNA pulldown kit (Thermo Fisher Scientific, China) was used to detect the interactions between HCP5 and miR-24-3p. The cells were lysed using TRIzol reagent, phenylmethylsulfonyl fluoride, and protease inhibitors. The biotinylated miR-24-3p probe and

streptavidin-coated magnetic beads were incubated with hybridisation buffer for 1 h. The mixture was incubated with lysis buffer for 4 h. The beads were washed with hybridisation buffer, the RNA bound to the beads was extracted, and RT-qPCR was performed to examine HCP5 expression.

2.17. RNA binding protein immunoprecipitation (RIP)

The hPDLSCs were collected and lysed. Cell lysates were incubated with magnetic beads conjugated to immunoglobulin G and Argonaute 2 antibody. RNA was extracted using TRIzol reagent and detected using PCR.

2.18. Enzyme-linked immunosorbent assay (ELISA)

The concentrations of tumour necrosis factor (TNF)-α, interleukin (IL)-1β, IL-6, and IL-8 in mice serum were measured using mice TNF-α, IL-1β, IL-6, IL-8 ELISA kit (Shanghai Enzyme-linked Biotechnology Co., Ltd., China). The concentrations of HO1 (Shanghai Enzyme-linked Biotechnology Co., Ltd., China) and carbon monoxide (CO; Shanghai Meiao Biotechnology Co., Ltd., China) in hPDLSCs were measured using human HO1 and CO ELISA kits. The supernatant of the mouse serum or cell culture was collected and centrifuged at 3000 rpm for 20 min to obtain the supernatant for later use. Then, 50 μL of different standard concentrations was added to the standard well. An equal volume of sample was added to each well. Then, 100 μL of horseradish peroxidase-labeled detection antibody

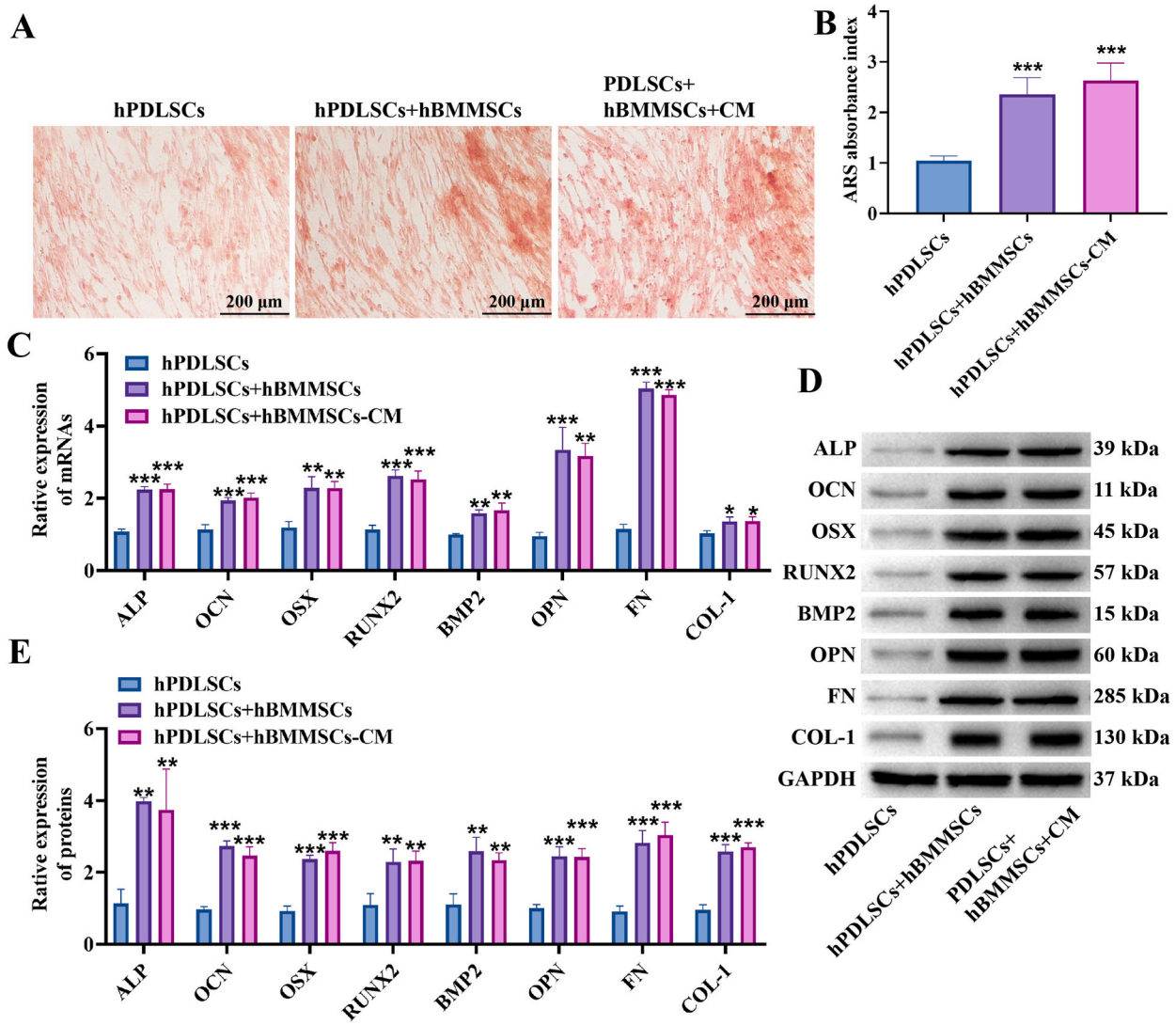

Fig. 1. Co-culture with hBMMSCs accelerated osteogenic differentiation of hPDLSCs. **A-B** ARS staining was performed to assess osteogenic differentiation (× 200). RT-qPCR (**C**) and Western blot (**D-E**) were used to detect the mRNAs and proteins expression of osteogenic markers ALP, OCN, OSX, RUNX2, BMP2, OPN, FN, and COL-1. $^{*}P < 0.05$, $^{**}P < 0.01$, $^{***}P < 0.001$ vs hPDLSCs group.

was added to each well and incubated for 60 min. After washing, the reaction solutions A and B were added and incubated in the dark for 15 min. After the reaction was terminated, the OD was measured at 450 nm.

2.19. Detection of heme, biliverdin, and Fe^{2+}

Heme, biliverdin, and Fe^{2+} detection kits (MERCK, China) were used to measure the concentrations of heme, biliverdin, and Fe^{2} in hPDLSCs following the manufacturer's protocol.

2.20. Statistical analysis

At least three biological replicates were performed in the above experiment, and each biological replicate of the RT-qPCR results included three technical replicates. The results were presented as "mean ± standard deviation". GraphPad Prism software was used to analyse the data and graphs. An independent-sample *t*-test was used for data comparison between two groups, and one-way analysis of variance was used for comparison among multiple groups. *P* less than 0.05 was considered to be statistically significant.

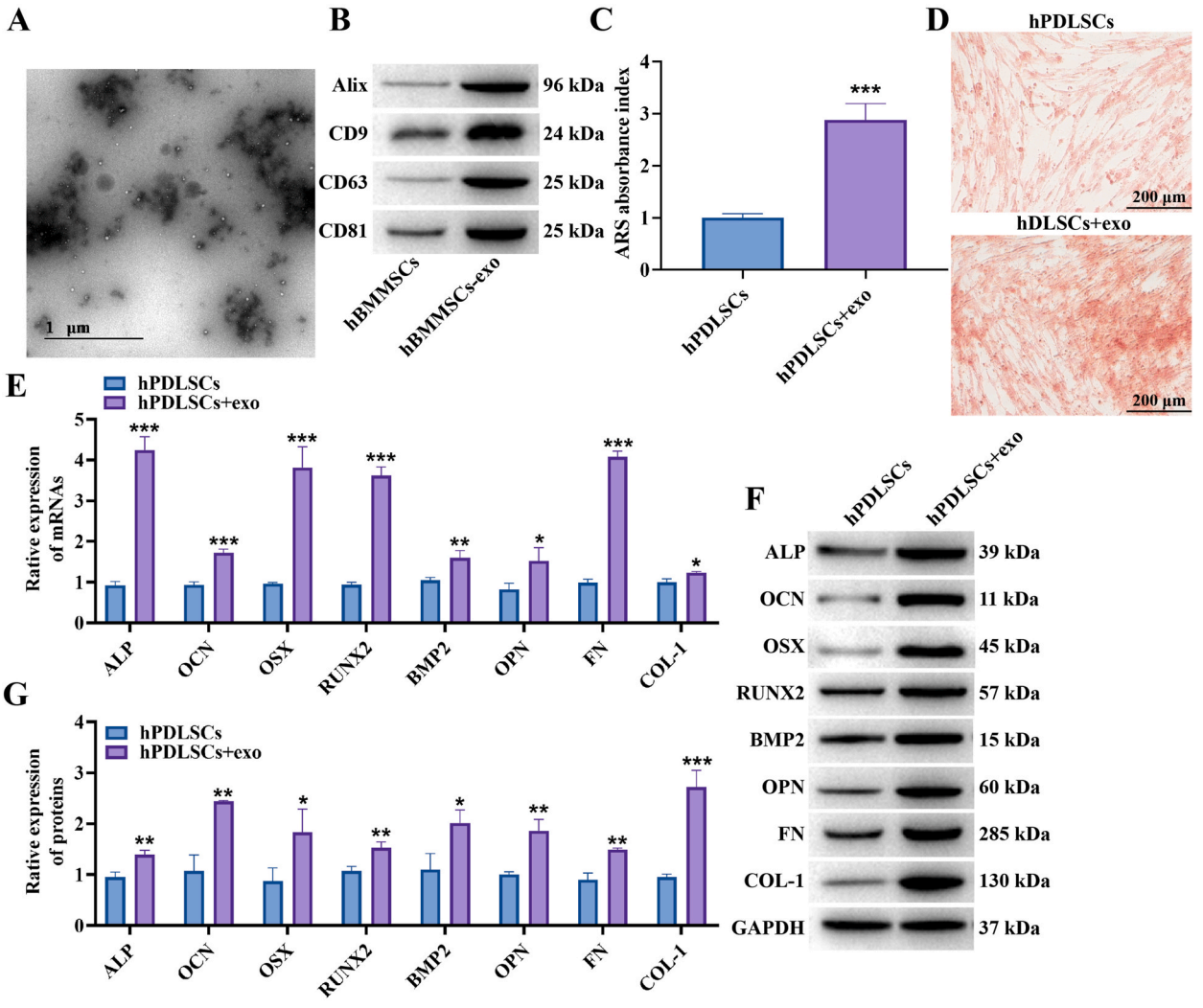

Fig. 2. hBMMSCs-derived exosomes promoted the osteogenic differentiation of hPDLSCs. **A** Exosomes was observed using TEM (× 30000). **B** The markers of exosomes were examined by Western blot. ***C*-D** ARS staining was performed to assess the osteogenic differentiation (× 200). RT-qPCR (**E**) and Western blot (**F-G**) were used to detect the mRNA and protein expression of osteogenic markers ALP, OCN, OSX, RUNX2, BMP2, OPN, FN, and COL-1. **P* < 0.05, ***P* < 0.01, ****P* < 0.001 vs hPDLSCs group.

3. Results

3.1. Co-culture with hBMMSCs accelerated the osteogenic differentiation of hPDLSCs

HBMMSCs were co-cultured with hPDLSCs, and ARS staining was performed to assess the osteogenic ability of hPDLSCs, the results are displayed in Fig. 1A. Compared with the PDLSCs group, the number of mineralised nodules in hPDLSCs co-cultured with hBMMSCs or the culture medium of hBMMSCs increased (Fig. 1B). RT-qPCR (Fig. 1C) and Western blot (Fig. 1D and E) were used to detect osteogenic markers, and the results indicated that the mRNA and protein levels of ALP, osteocalcin (OCN), osterix (OSX), runt-related transcription factor 2 (RUNX2), bone morphogenetic protein 2 (BMP2), osteopontin (OPN), fibronectin (FN), and collagen 1 (COL-1)

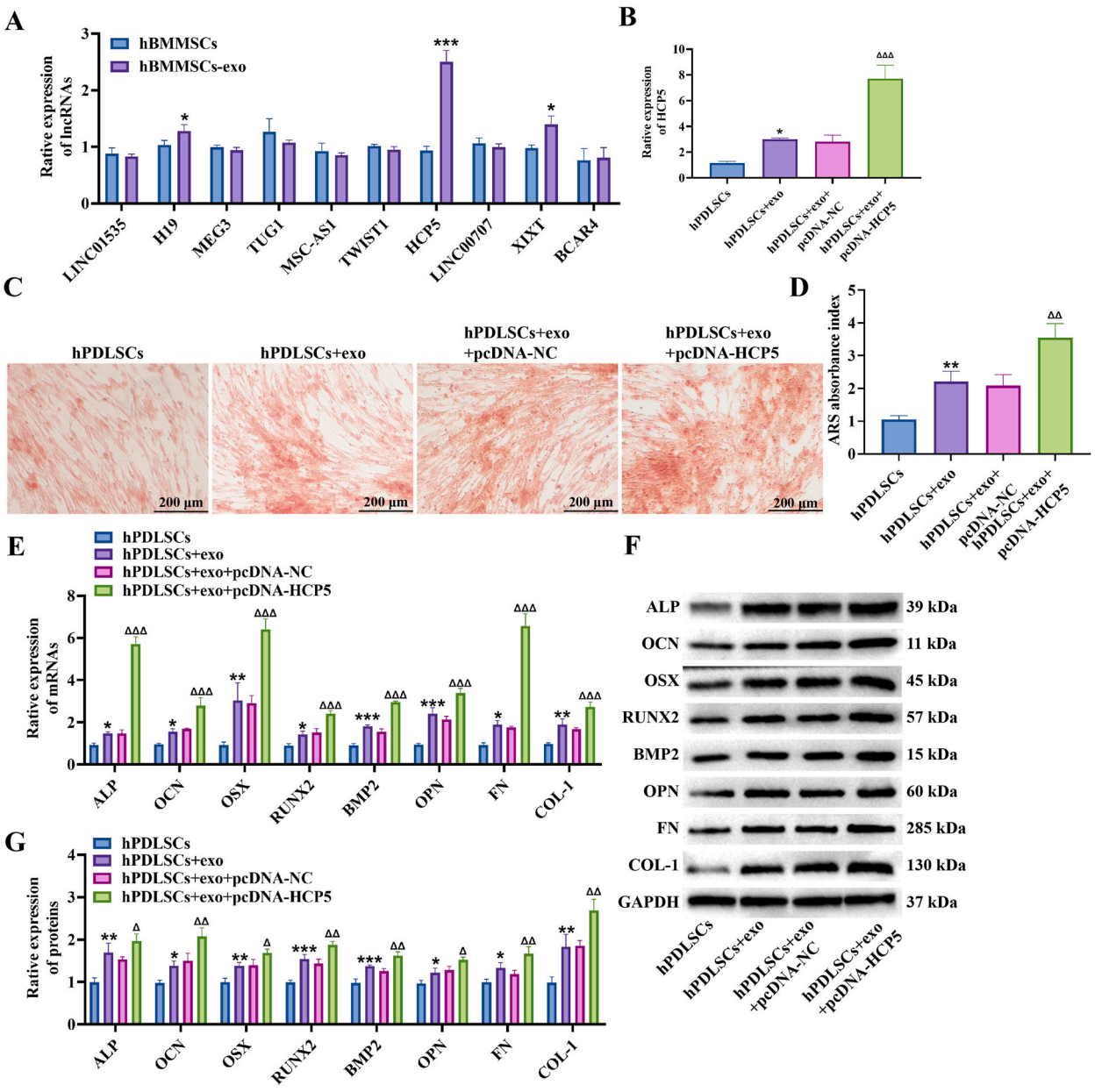

Fig. 3. hBMMSCs-derived exosomal HCP5 enhanced the osteogenic differentiation of hPDLSCs. **A** The expression of lncRNA was determined using RT-qPCR, $^{*}P < 0.05$, $^{***}P < 0.001$ vs hBMMSCs group. **B** RT-qPCR was used to test the expression of HCP5. ***C*-D** ARS staining was performed to assess the osteogenic differentiation (× 200). RT-qPCR **(E)** and Western blot **(F-G)** were used to detect the mRNA and protein expression of osteogenic markers ALP, OCN, OSX, RUNX2, BMP2, OPN, FN, and COL-1. $^{*}P < 0.05$, $^{**}P < 0.01$, $^{***}P < 0.001$ vs hPDLSCs group. $^{\triangle}P < 0.05$, $^{\triangle\triangle}P < 0.01$, $^{\triangle\triangle\triangle}P < 0.001$ vs hPDLSCs + exo + pcDNA-NC group.

were significantly increased in the hPDLSCs + hBMMSCs and hPDLSCs + hBMMSCs-CM groups compared with than those in the hPDLSCs group. Therefore, the above results indicate that hBMMSCs and hBMMSCs-CM increased osteogenesis in hPDLSCs.

3.2. HBMMSCs-derived exosomes promoted the osteogenic differentiation of hPDLSCs

Next, we extracted exosomes from hBMMSCs, and TEM observation revealed the typical cup-shaped structure of the exosomes (Fig. 2A). The markers of exosomes, Alix, CD9, CD63, and CD81 were overexpressed in hBMMSCs-exo compared with hBMMSCs (Fig. 2B). ARS staining revealed that the matrix mineralisation of hPDLSCs co-cultured with hBMMSCs-exo significantly increased (Fig. 2C and D). Concurrently, in the hBMMSCs-exo group, the expression of ALP, OCN, OSX, RUNX2, BMP2, OPN, FN, and COL-1 mRNAs (Fig. 2E) and proteins (Fig. 2F and G) increased in comparison with the hPDLSCs single culture group. These results indicate that hBMMSCs derived exosomes accelerate the osteogenic ability of hPDLSCs.

3.3. hBMMSCs exosome-derived HCP5 enhanced the osteogenic differentiation of hPDLSCs

LINC01535 [17], H19 [5], MEG3 [18], TUG1 [19], MSC-AS1 [20], TWIST1 [21], HCP5 [22], LINC00707 [23], XIST [24], and

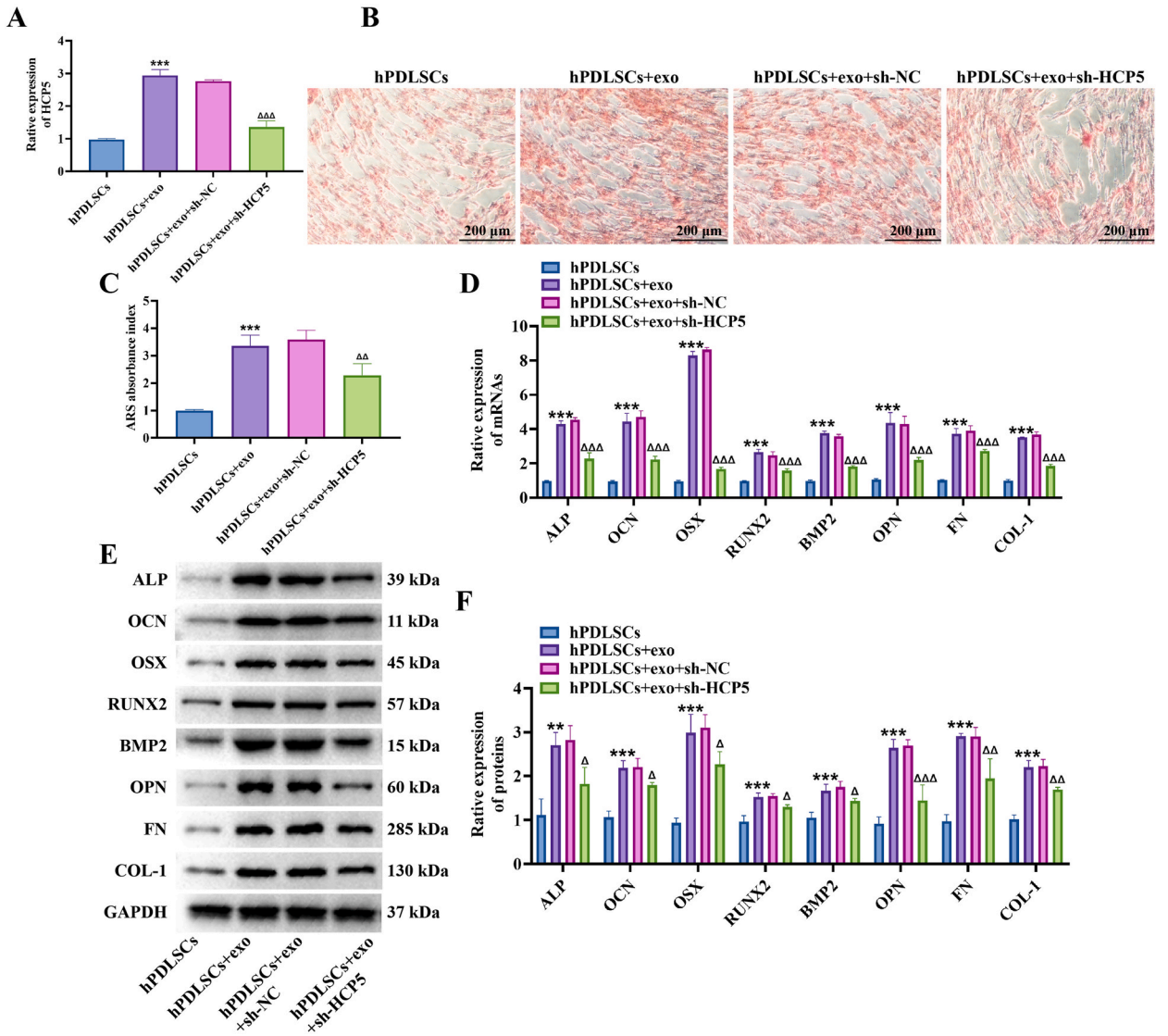

Fig. 4. Knocking down HCP5 inhibited the osteogenic differentiation of hPDLSCs. **A** The expression of HCP5 was determined using RT-qPCR. **B–C** ARS staining was performed to assess the osteogenic differentiation (× 200). RT-qPCR **(D)** and **(E-F)** Western blot was used to detect the mRNAs and proteins expression of osteogenic markers ALP, OCN, OSX, RUNX2, BMP2, OPN, FN, and COL-1. $^{**}P < 0.01$, $^{***}P < 0.001$ vs hPDLSCs group. $^{\triangle}P < 0.05$, $^{\triangle\triangle}P < 0.01$, $^{\triangle\triangle\triangle}P < 0.001$ vs hPDLSCs + exo + sh-NC group.

BCAR4 [25] are involved in osteogenic differentiation. In the present study, we examined the expression of these lncRNAs. These results suggested that H19, HCP5, and XIST expression levels were higher in the hBMMSCs-exo group than in the hBMMSCs group (Fig. 3A). Compared with their respective control groups, the expression of HCP5 was the most significant. Therefore, HCP5 was selected for further analyses. HBMMSCs were transfected with pcDNA-HCP5, and exosomes were isolated from hBMMSCs and co-cultured with hPDLSCs. RT-qPCR assay revealed that compared with the hPDLSCs group, HCP5 was overexpressed in the hPDLSCs + exo group (Fig. 3B), transfection with pcDNA-HCP5 promoted HCP5 expression. ARS staining results are displayed in Fig. 3C and D, overexpression of HCP5 increased the matrix mineralisation of hPDLSCs. Moreover, the mRNAs (Fig. 3E) and proteins (Fig. 3F and G) levels of ALP, OCN, OSX, RUNX2, BMP2, OPN, FN, and COL-1 were upregulated in the HCP5 overexpression group.

Next, sh-NC and sh-HCP5 were transfected into hBMMSCs. The RT-qPCR results revealed that transfection with sh-HCP5 inhibited HCP5 expression (Fig. 4A). HCP5 inhibition decreased the matrix mineralisation of hPDLSCs (Fig. 4B and C). The expression of ALP, OCN, OSX, RUNX2, BMP2, OPN, FN, and COL-1 mRNAs (Fig. 4D) and proteins (Fig. 4E and F) were inhibited by downregulation of HCP5. These results indicate that overexpression of HCP5 in hBMMSCs-derived exosomes enhanced the osteogenic ability of hPDLSCs, and downregulation of HCP5 inhibited the osteogenic differentiation of hPDLSCs.

3.4. Downregulation of HCP5 in hBMMSCs exosomes promoted the inflammation response and repressed the osteogenic differentiation of CP mouse

To further explore the effect of HCP5 on CP mouse, we induced a CP mouse model by wrapping around the gingival sulcus of the bilateral maxillary second molars and injecting hBMMSCs exosomes into the periodontium of the experimental teeth of CP mice. Micro-CT detection showed that in the CP group, alveolar bone resorption and the CEJ-ABC distance increased (Fig. 5A). However, after treatment with exo-sh-NC, the CEJ-ABC of mice decreased. CEJ-ABC was higher in the HCP5 inhibition group than in the exo-sh-

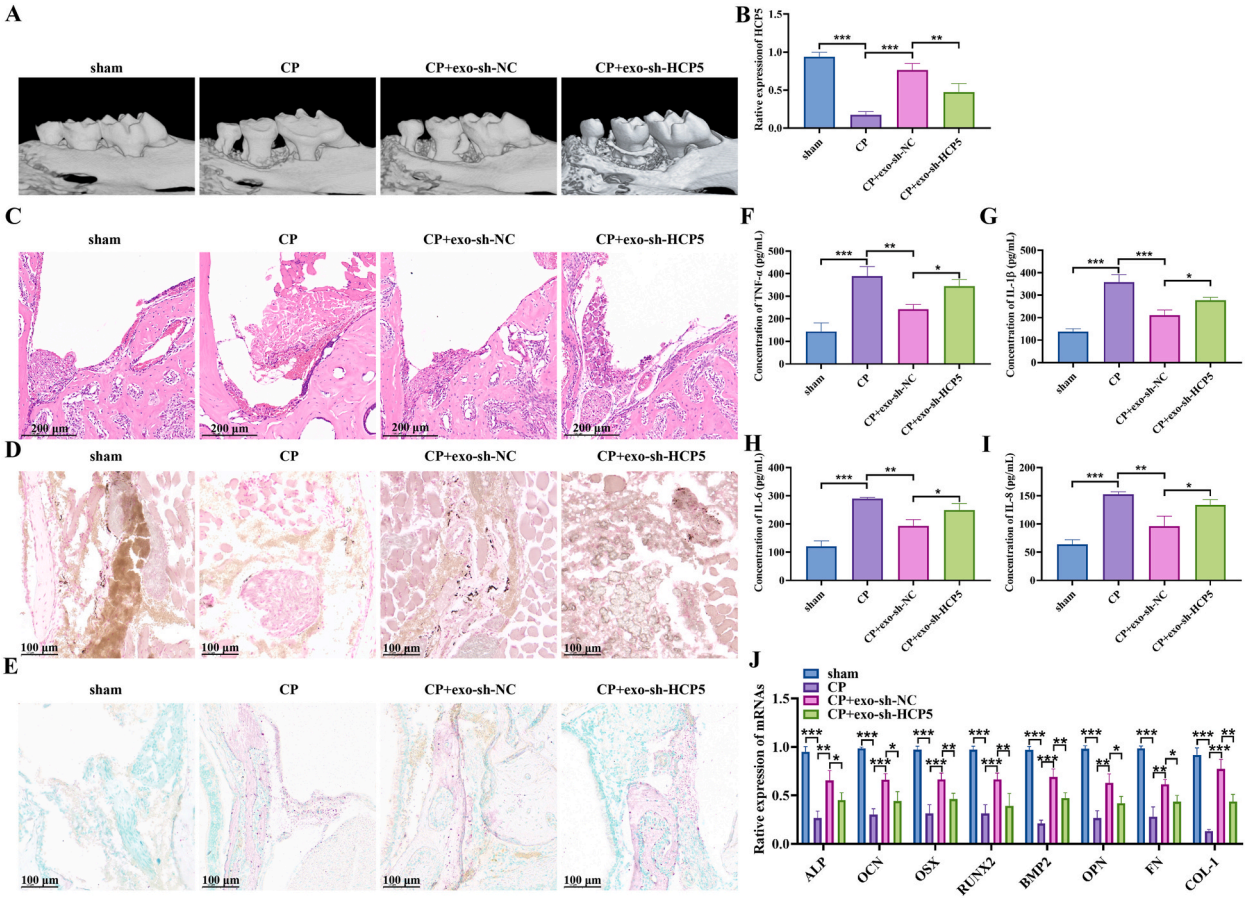

Fig. 5. Downregulation of HCP5 in hBMMSCs exosomes promoted the inflammation and repressed the osteogenic differentiation of CP mouse. **A** Micro-CT was carried out to observe the periodontal defect of mouse. **B** RT-qPCR was used to measure HCP5 level. **C** HE staining was performed to observe the pathological damage (× 15). **D** ALP staining was used to assess the osteogenic differentiation (× 20). **E** TRAP staining was used to evaluate the osteoclast differentiation (× 20). **F–I** ELISA kits were used to examine the concentration of cytokines. **J**. The expressions of osteogenic markers *ALP*, *OCN*, *OSX*, *RUNX2*, *BMP2*, *OPN*, *FN*, and *COL*-1 mRNA were assessed using RT-qPCR assay. *$P < 0.05$, **$P < 0.01$, ***$P < 0.001$ represented significant differences among the indicated group.

NC group. RT-qPCR assays revealed that HCP5 was inhibited in CP mice, exosomes transfected with sh-NC increased HCP5 expression, and exosomes transfected with sh-HCP5 significantly decreased HCP5 expression (Fig. 5B).

HE (Fig. 5C), ALP (Fig. 5D), and TRAP (Fig. 5E) staining indicated that the inflammatory infiltration in CP mice was significant, the number of osteoblasts decreased, and the number of osteoclasts increased. In the exo-sh-NC group, inflammatory infiltration was relieved, the number of osteoblasts increased, and the number of osteoclasts decreased. Knockdown of HCP5 had the opposite effect than in the exo-sh-NC group. The ELISA results are shown in Fig. 5F–I. The concentration of pro-inflammatory cytokines TNF-α, IL-1β, IL-6, and IL-8 was higher in the CP group than those in the sham group. Treatment with exo-sh-NC repressed pro-inflammatory cytokines levels compared with CP group. HCP5 inhibition increased the levels of pro-inflammatory cytokines than those in exo-sh-NC group. The osteogenic markers *ALP*, *OCN*, *OSX*, *RUNX2*, *BMP2*, *OPN*, *FN*, and *COL*-1 mRNAs levels decreased in CP mice (Fig. 5J), whereas exo-sh-NC increased their expression, and knockdown of HCP5 in exosomes had the opposite effects on the exo-sh-NC group. These results indicated that HCP5 knockdown promoted the inflammatory response and repressed osteogenic differentiation in CP mice.

3.5. HCP5 targeted miR-24-3p and regulated HO1 expression

LncTar database was used to predict the binding sequences between HCP5 and miR-24-3p (Fig. 6A). A dual luciferase reporter assay revealed that the miR-24-3p mimic suppressed the luciferase activity of HCP5-WT (Fig. 6B) but had no obvious inhibitory effect on the luciferase activity of HCP5-MUT. RT-qPCR revealed that HCP5 overexpression decreased the miR-24-3p expression (Fig. 6C). To further verify the interaction between HCP5 and miR-24-3p, we conducted an RNA pulldown assay and found that the miR-24-3p probe significantly pulled down HCP5 (Fig. 6D). RIP experiments revealed that HCP5 and miR-24-3p were enriched in the anti-

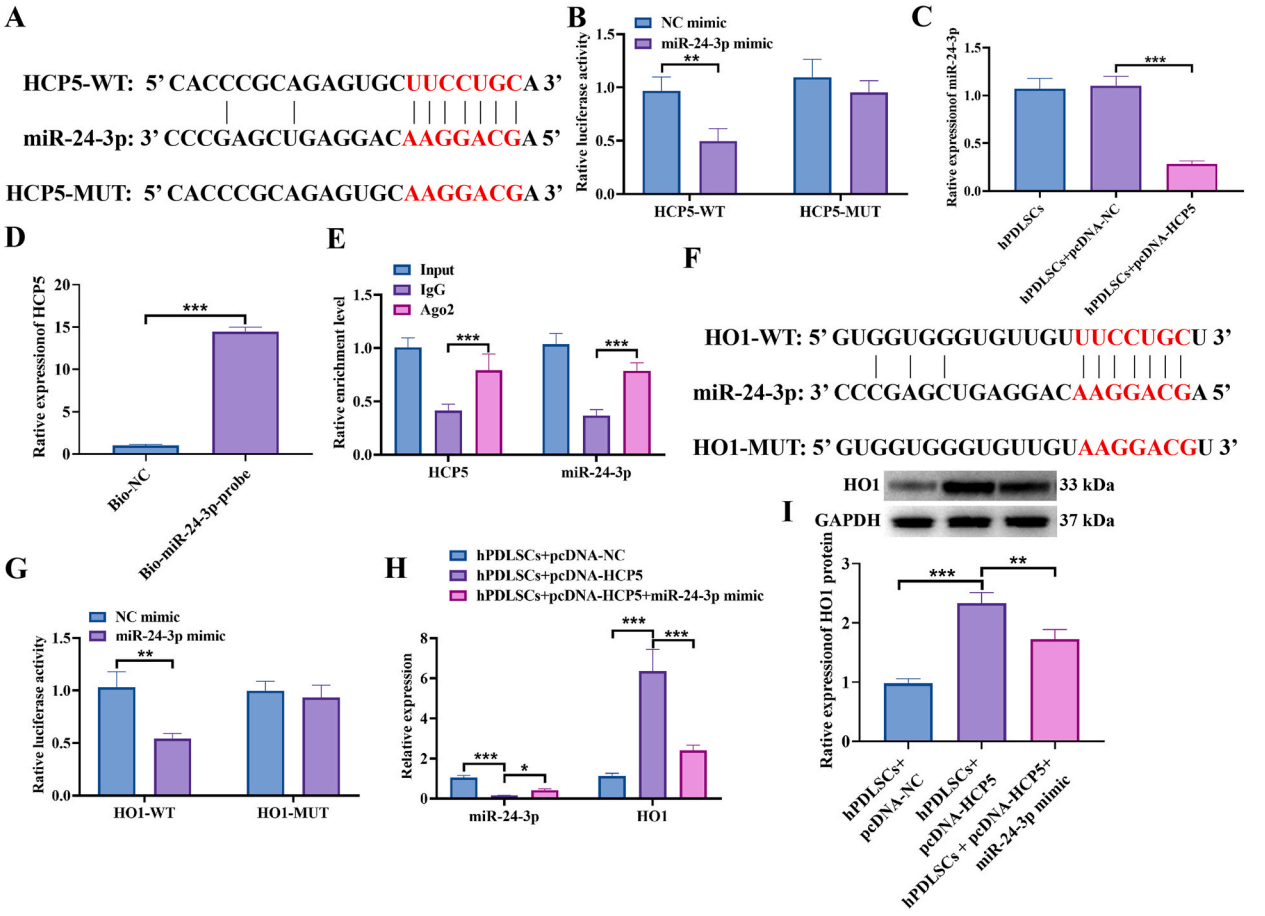

Fig. 6. HCP5 targeted miR-24-3p and regulated *HO1* expression. **A** The binding sequences between HCP5 and miR-24-3p. **B** Dual luciferase reporter analyzed the interaction between HCP5 and miR-24-3p. **C** miR-24-3p expression was examined by RT-qPCR assay. **D**. RT-qPCR assay analyzed the HCP5 expression retrieved by biotin-labeled miR-24-3p. **E**. RIP-PCR experiment was used to identify the interaction between HCP5 and miR-24-3p. **F** The binding sequences between miR-24-3p and HO1. **G** Dual luciferase reporter analyzed the interaction between miR-24-3p and HO1. **H** miR-24-3p and *HO1* mRNA expression was detected by RT-qPCR assay. **I** Western blot evaluated HO1 protein expression. *$P < 0.05$, **$P < 0.01$, ***$P < 0.001$ represented significant differences among the indicated group.

Argonaute 2 antibody group (Fig. 6E).

Then, the starbase database was used to predict the target of miR-24-3p, and HO1 3′UTR was found to be bound to miR-24-3p (Fig. 6F). The dual luciferase assay indicated that miR-24-3p mimic significantly repressed HO1-WT luciferase activity (Fig. 6G) but had no obvious inhibitory effect on the luciferase activity of HO1-MUT. Increased HCP5 expression inhibited miR-24-3p and upregulated *HO1* mRNA expression (Fig. 6H). The miR-24-3p mimic reversed the effect of increased HCP5 on miR-24-3p and *HO1* mRNA. Western blot revealed that HCP5 upregulation increased HO1 protein levels (Fig. 6I) in hPDLSCs and that the miR-24-3p mimic repressed HO1expression.

3.6. hBMMSCs-derived exosomal HCP5 regulated hPDLSCs osteogenic differentiation by sponging miR-24-3p/HO1

To further understand the function of the HCP5/miR-24-3p/*HO1* axis in the osteogenic differentiation of hPDLSCs, we transfected pcDNA-HCP5 into hBMMSCs, isolated exosomes, co-cultured the exosomes with hPDLSCs, and transfected the NC mimic and miR-24-3p mimic into hPDLSCs. Western blot was performed to evaluate HO1 expression, and the results indicated that transfection of pcDNA-HCP5 upregulated HO1 protein (Fig. 7A), while HO1 protein was inhibited by transfection of pcDNA-HCP5 and miR-24-3p mimic.

Osteogenic markers were assessed using Western blot (Fig. 7B and C), and found that ALP, OCN, OSX, RUNX2, BMP2, OPN, FN, and COL-1 protein levels increased in the HCP5 upregulation group, but decreased by miR-24-3p upregulation. ARS staining suggested that HCP5 overexpression promoted the formation of mineralised nodules (Fig. 7D and E). However, miR-24-3p upregulation decreased the formation of mineralised nodules. These results revealed that hBMMSCs-derived exosomal HCP5 acted as a sponge for miR-24-3p, increased *HO1* expression, and accelerated the osteogenic differentiation of hPDLSCs.

3.7. Increased HO1 accelerated osteogenic differentiation of hPDLSCs by activating P38/ELK1 pathway

HO1 is an essential enzyme in heme catabolism, and the *P38/ELK1* pathway is involved in osteogenic differentiation [26]. We speculated that *HO1* regulates heme decomposition and CO production, which mediates the activation of the *P38/ELK1* signalling pathway and regulates osteogenic differentiation. To investigate whether *HO1* regulates the osteogenic differentiation of hPDLSCs through the *P38/ELK1* signalling pathway, we transfected pcDNA-NC and pcDNA-HO1 into hPDLSCs and treated hPDLSCs with PD169316. The RT-qPCR results showed that overexpression of *HO1* promoted *HO1* (Fig. 8A), *P38* (Fig. 8B), and *ELK1* (Fig. 8C) mRNA expression. Overexpression of *HO1* and treatment with PD169316 had no significant effect on *HO1*, *P38*, and *ELK1* mRNAs expression compared with the *HO1* overexpression group.

Kits were used to measure the concentrations of heme, biliverdin, and Fe^{2+}. Overexpression of *HO1* decreased heme concentration (Fig. 8D) and promoted the production of biliverdin (Fig. 8E) and Fe^{2+} (Fig. 8F). The ELISA results showed that *HO1* overexpression

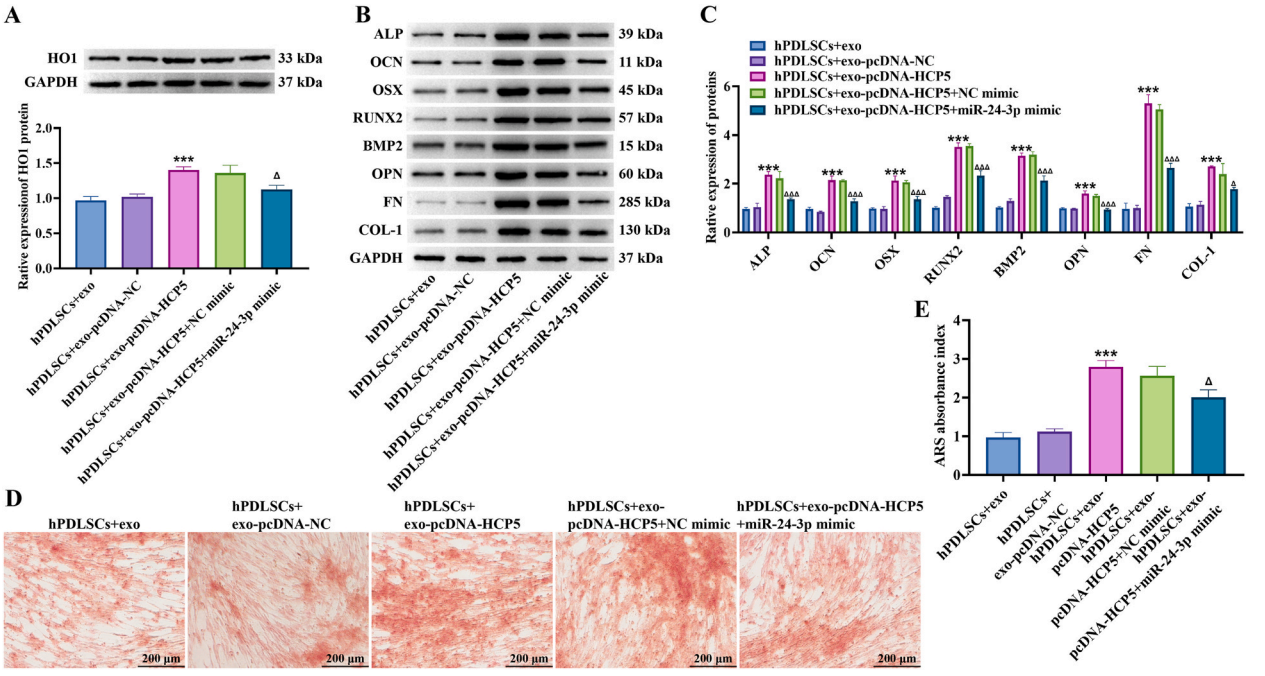

Fig. 7. hBMMSCs-derived exosomal HCP5 regulated hPDLSCs osteogenic differentiation by regulating miR-24-3p/*HO1*. **A** Western blot measured HO1 protein level. **B–C** Western blot was carried out to assess osteogenic markers ALP, OCN, OSX, RUNX2, BMP2, OPN, FN, and COL-1 protein expression. **D-E** ARS staining assessed the osteogenic ability of hPDLSCs (× 200). ***$P < 0.001$ vs hPDLSCs + exo-pcDNA-NC group. $^{\triangle}P < 0.05$, $^{\triangle\triangle\triangle}P < 0.001$ vs hPDLSCs + exo + pcDNA-HCP5+NC mimic group.

enhanced HO1 (Fig. 8G) and CO levels (Fig. 8H). Western blot was conducted to evaluate the protein levels of HO1, P38, P–P38, ELK1, and P-ELK1 (Fig. 8I and J); increased HO1 upregulated HO1, P38, P–P38, ELK1, and P-ELK1 proteins. PD169316 treatment significantly reduced P–P38 and P-ELK1 expression. RT-qPCR and ARS staining assays revealed that *HO1* overexpression promoted *ALP*, *OCN*, *OSX*, *RUNX2*, *BMP2*, *OPN*, *FN*, and *COL*-1 mRNAs expression (Fig. 8K) and increased the number of mineralised nodules (Fig. 8L-M) in hPDLSCs. However, treatment with PD169316 significantly repressed *ALP*, *OCN*, *OSX*, *RUNX2*, *BMP2*, *OPN*, *FN*, and *COL*-1 mRNAs expression and the mineralised nodules of hPDLSCs. These results indicated that *HO1* promotes heme decomposition and the osteogenic differentiation of hPDLSCs by releasing CO and activating the *P38/ELK1* signalling pathway.

4. Discussion

CP affects oral health and aggravates the development of systemic diseases. Simultaneously, the severity of CP increases with age, thus exerting a greater impact on the health of older people. In clinical practice, CP is often treated with basic treatment, drugs, and surgery. The periodontal environment inhibits PDLSCs regeneration and aggravates the destruction of periodontal tissues. Therefore, studying the potential molecular mechanisms of inhibiting periodontitis and promoting the osteogenic differentiation of PDLSCs is expected to provide new ideas for treating and preventing CP. In this study, we demonstrated that the hBMMSCs-derived exosomal HCP5 enhanced the osteogenic differentiation of hPDLSCs and alleviated CP in mice by regulating the miR-24-3p*/HO1/P38/ELK1* signalling pathway.

Exosomes are ingested by target cells through the exocytosis of donor cells and transmit biological signals between cells. BMMSCs exosomes are some of the most widely studied exosomes and have been shown to be involved in the regulating various biological processes, especially osteogenic differentiation [3,27,28]. For example, bone marrow mesenchymal stem cells-derived exosomal miR-424-5p attenuated osteogenic development by inhibiting WNT inhibitory factor 1 and activating the Wnt/β-catenin pathway [27]. Bone marrow-derived mesenchymal stem cell-secreted exosomal lncRNA metastasis-associated lung adenocarcinoma transcript 1 increases osteoblast activity and alleviates osteoporosis by mediating miR-34c/special AT-rich sequence-binding protein 2 axes [3]. Herein, we found that HCP5 was overexpressed in hBMMSCs-secreted exosomes, overexpression of HCP5 promoted the osteogenic ability of hPDLSCs, and HCP5 inhibition inhibited the osteogenic differentiation of hPDLSCs. HCP5 knockdown in hBMMSCs exosomes increased inflammatory cytokines levels and reduced osteogenesis in CP mice. Li et al. reported that HCP5 from BMMSCs-exosomes

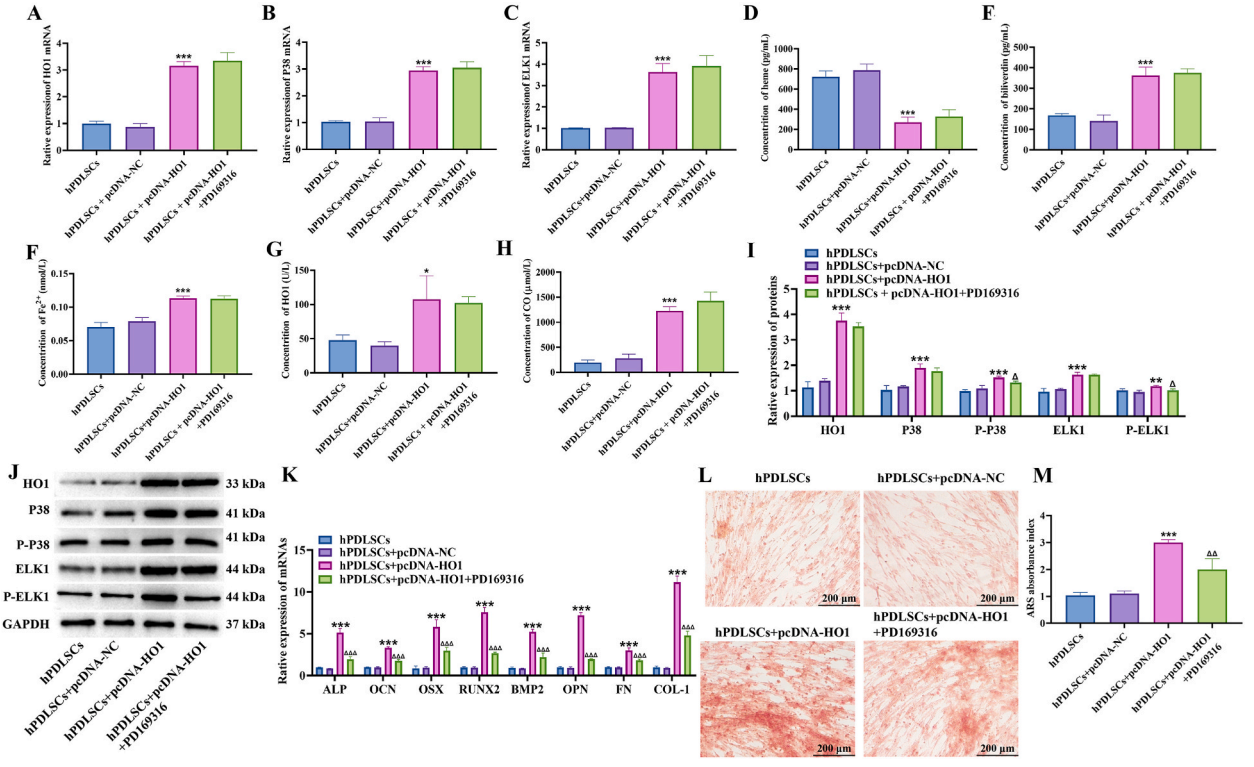

Fig. 8. Increased *HO1* promoted CO release and accelerated the osteogenic differentiation of hPDLSCs by activating *P38/ELK1* pathway. RT-qPCR analyzed the mRNAs expression of *HO1* (**A**), *P38* (**B**), and *ELK1* (**C**). Detection kits were used to detected the concentration of heme (**D**), biliverdin (**E**), and Fe^{2+} (**F**). ELISA kits detected HO1 (**G**) and CO (**H**) concentration. **I-J** Western blot was performed to measure the proteins expression of HO1, P38, P–P38, ELK1, and P-ELK1. **K** RT-qPCR was carried out to test osteogenic markers *ALP*, *OCN*, *OSX*, *RUNX2*, *BMP2*, *OPN*, *FN*, and *COL*-1 mRNAs expression. **L-M** ARS staining evaluated the osteogenic ability of hPDLSCs (× 200). $^{**}P < 0.01$, $^{***}P < 0.001$ vs hPDLSCs + pcDNA-NC group. $^{\triangle}P < 0.05$, $^{\triangle\triangle}P < 0.01$ and $^{\triangle\triangle\triangle}P < 0.001$ vs hPDLSCs + pcDNA-HO1 group.

protects cardiomyocytes against ischaemia-reperfusion injury [10]. Overexpression of HCP5 in human umbilical cord mesenchymal stem cells promotes proliferation and inhibits apoptosis in ovarian granulosa cells [29].

Studies have shown that HCP5 exerts a wide range of regulatory effects on tumour cells. In gastric cancer [7], neuroblastoma [8], multiple myeloma [12], nasopharyngeal carcinoma [30], pancreatic cancer [31], cervical cancer [32], colon cancer [33], acute myeloid leukemia [34], esophageal carcinoma [35], and laryngeal squamous cell carcinoma [17,36], the expression of HCP5 is significantly upregulated and accelerates cancer development. In ischaemia-reperfusion injury, HCP5 overexpression increases the viability of myocardial cells and reduces apoptosis after hypoxia-reperfusion, thus alleviating myocardial ischaemia-reperfusion injury [37]. However, increased HCP5 expression exacerbates cerebral ischaemia-reperfusion injury by sponging miR-652-3p [38]. Moreover, HCP5 represses allergic rhinitis by promoting the differentiation and proliferation of regulatory T cells [9].

miR-24-3p is a short-chain noncoding RNA. Several studies have shown that miR-24-3p plays a regulatory role in tumours as both a cancer-promoting and cancer-inhibiting factor, such as in prostate cancer [39], lung cancer [40], and breast cancer [41]. miR-24-3p is also involved in the regulation of osteogenesis. Decreased miR-24-3p expression suppresses osteogenic differentiation of dental pulp stem cells [42]. miR-24-3p inhibits osteogenic differentiation of human adipose-derived mesenchymal stem cells [43]. In this study, we found that miR-24-3p was a target of HCP5 and overexpression of miR-24-3p inhibited the formation of mineralised nodules and decreased the expression of ALP, OCN, OSX, RUNX2, BMP2, OPN, FN, and COL-1 proteins in hPDLSCs. This is consistent with the results reported by pang et al. [44]. In addition, we found that miR-24-3p targeted *HO1*, and negatively regulated *HO1* expression.

HO1 is an important rate-limiting enzyme in heme metabolism. The heme releases biliverdin, Fe^{2+}, and CO under the catalysis of *HO1*, and biliverdin is reduced to bilirubin by biliverdin reductase. Biliverdin and bilirubin exhibit anti-inflammatory and antioxidant effects. CO is an important gaseous messenger in the body, and has anti-inflammatory and anti-apoptotic effects. *HO1* plays an important role in bone formation. Verheijen et al. [45] found that *HO1* was highly expressed in the ALP-positive region of the palatal mesenchyme derived from cranial neural crest cells. Upregulated *HO1* promotes proliferation and osteogenic differentiation of bone marrow stromal cells [46]. Inhibition of *HO1* suppresses the expression of osteogenic marker genes and osteoblast differentiation [47]. Herein, we found that overexpressed *HO1* decreased heme levels, promoted the release of biliverdin, Fe^{2+}, and CO and accelerated the osteogenesis of hPDLSCs. Moreover, upregulation of *HO1* activated the *P38/ELK1* signalling pathway.

P38 mitogen-activated protein kinase (MAPK) is an important member of the MAPK family. Various extracellular stimuli can lead to the phosphorylation of P38 MAPK and activation of the *P38/MAPK* signalling pathway. ELK1 is a member of the ETS family that can be phosphorylated and activated by MAP*K* [48]. Studies have found that the *P38/ELK1* pathway is involved in many biological processes [49]. Zou et al. [50] showed that asprosin inhibits lipid accumulation in macrophages, diminishes the atherosclerotic area, improves plasma lipid profiles, and facilitates reverse cholesterol transport by activating the *P38/ELK1* signalling pathway. Activation of the *P38* pathway increases the osteogenic ability of mesenchymal stem cells [51]. In this study, we found that treatment with PD169316 significantly decreased the number of mineralised nodules and the expression of osteogenic markers in hPDLSCs.

In conclusion, our results indicate that hBMMSCs-derived exosomal HCP5, as a sponge of miR-24-3p, promotes the osteogenic differentiation of hPDLSCs by promoting *HO1* expression and activating the *P38/ELK1* signalling pathway. Therefore, HCP5 is a potential target for the treatment of CP. However, this study has some limitations. We hypothesised that *HO1* promotes the decomposition of heme into CO, activates the *P38/ELK1* signalling pathway, and then regulates the osteogenic differentiation of hPDLSCs; however, the mechanism between CO and the *P38* signalling pathway and its effect on osteogenic differentiation of hBMMSCs needs to be further explored. In addition, other studies have also reported the potential therapeutic target of CP. We also previously found that miR-335-3p derived from hBMMSCs exosomes promoted the osteogenic differentiation of hPDLSCs and alleviated periodontitis by inhibiting DKK1 expression [52]. Combined with the results of this study, we believe that there may be multiple RNA regulation mechanisms to mediate the osteogenic differentiation of hPDLSCs in CP. Whether HCP5 is the key therapeutic target of CP still needs a lot of research to be determined.

Funding

This study was supported by Joint Project of Applied Basic Research of Kunming Medical University and Yunnan Provincial Science and Technology Department (No. 202001AY070001-254 (Xiao-hong Yu), No. 202101AY070001-193 (Yu Liu), and No. 2019FE001 (−251) (Jin Zhu)) and the Medicine Leading Talent of Yunnan Province Health Care Committee (No. L-201801 (Wei-hong Wang)).

Ethics declarations

This study was approved by the Laboratory Animal Ethics Committee of Yunnan Labreal Biotechnology Co., Ltd, with the approval number PZ20211113.

Data availability statement

Data included in article/supp. material/referenced in article.

CRediT authorship contribution statement

Yu Liu: Writing – original draft, Funding acquisition, Conceptualization. **Jin Zhu:** Writing – original draft, Validation, Methodology, Funding acquisition. **Wei-hong Wang:** Validation, Methodology, Funding acquisition. **Lian Zeng:** Validation, Methodology.

Yan-ling Yang: Validation, Methodology. **Zhou Wang:** Visualization, Software, Data curation. **Jian-qi Liu:** Visualization, Software, Data curation. **Wei Li:** Visualization, Software, Data curation. **Jing-yu Sun:** Visualization, Software, Data curation. **Xiao-hong Yu:** Writing – review & editing, Funding acquisition, Conceptualization.

Declaration of competing interest

The authors declare that they have no known competing financial interests or personal relationships that could have appeared to influence the work reported in this paper.

Acknowledgments

We are grateful to Hui Li and the experimental animal team of Yunnan Labreal Biotechnology Co., Ltd. for providing technical support in constructing mouse model of this work.

Appendix A. Supplementary data

Supplementary data to this article can be found online at https://doi.org/10.1016/j.heliyon.2024.e34203.

References

[1] J.J. Segura-Egea, J. Martín-González, L. Castellanos-Cosano, Endodontic medicine: connections between apical periodontitis and systemic diseases, Int. Endod. J. 48 (10) (2015) 933–951.
[2] M.O. Freire, A. Devaraj, A. Young, et al., A bacterial-biofilm-induced oral osteolytic infection can be successfully treated by immuno-targeting an extracellular nucleoid-associated protein, Mol Oral Microbiol 32 (1) (2017) 74–88.
[3] X. Yang, J. Yang, P. Lei, et al., LncRNA MALAT1 shuttled by bone marrow-derived mesenchymal stem cells-secreted exosomes alleviates osteoporosis through mediating microRNA-34c/SATB2 axis, Aging (Albany NY) 11 (20) (2019) 8777–8791.
[4] S. Chen, Y. Tang, Y. Liu, et al., Exosomes derived from miR-375-overexpressing human adipose mesenchymal stem cells promote bone regeneration, Cell Prolif. 52 (5) (2019) e12669.
[5] J. Behera, A. Kumar, M.J. Voor, et al., Exosomal lncRNA-H19 promotes osteogenesis and angiogenesis through mediating Angpt1/Tie2-NO signaling in CBS-heterozygous mice, Theranostics 11 (16) (2021) 7715–7734.
[6] Y. Chen, Y. Wu, L. Guo, et al., Exosomal Lnc NEAT1 from endothelial cells promote bone regeneration by regulating macrophage polarization via DDX3X/NLRP3 axis, J. Nanobiotechnol. 21 (1) (2023) 98.
[7] H. Wu, B. Liu, Z. Chen, et al., MSC-induced lncRNA HCP5 drove fatty acid oxidation through miR-3619-5p/AMPK/PGC1α/CEBPB axis to promote stemness and chemo-resistance of gastric cancer, Cell Death Dis. 11 (4) (2020) 233.
[8] K. Zhu, L. Wang, X. Zhang, et al., LncRNA HCP5 promotes neuroblastoma proliferation by regulating miR-186-5p/MAP3K2 signal axis, J. Pediatr. Surg. 56 (4) (2021) 778–787.
[9] C. Yang, C. Shangguan, C. Cai, et al., LncRNA HCP5 participates in the tregs functions in allergic rhinitis and drives airway mucosal inflammatory response in the nasal epithelial cells, Inflammation 45 (3) (2022) 1281–1297.
[10] K.S. Li, Y. Bai, J. Li, et al., LncRNA HCP5 in hBMSC-derived exosomes alleviates myocardial ischemia reperfusion injury by sponging miR-497 to activate IGF1/PI3K/AKT pathway, Int. J. Cardiol. 342 (2021) 72–81.
[11] X. Wang, Y. Liu, J. Rong, et al., LncRNA HCP5 knockdown inhibits high glucose-induced excessive proliferation, fibrosis and inflammation of human glomerular mesangial cells by regulating the miR-93-5p/HMGA2 axis, BMC Endocr. Disord. 21 (1) (2021) 134.
[12] Q. Liu, R. Ran, M. Song, et al., LncRNA HCP5 acts as a miR-128-3p sponge to promote the progression of multiple myeloma through activating Wnt/β-catenin/cyclin D1 signaling via PLAGL2, Cell Biol. Toxicol. 38 (6) (2022) 979–993.
[13] M.L. Luo, Y. Jiao, W.P. Gong, et al., Macrophages enhance mesenchymal stem cell osteogenesis via down-regulation of reactive oxygen species, J. Dent. 94 (2020) 103297.
[14] L. Gan, L. Zhong, Z. Shan, et al., Epigallocatechin-3-gallate induces apoptosis in acute promyelocytic leukemia cells via a SHP-1-p38α MAPK-Bax cascade, Oncol. Lett. 14 (5) (2017) 6314–6320.
[15] Y. Nishiki, A. Adewola, M. Hatanaka, et al., Translational control of inducible nitric oxide synthase by p38 MAPK in islet β-cells, Mol. Endocrinol. 27 (2) (2013) 336–349.
[16] L. Xue, X. Zou, X.Q. Yang, et al., Chronic periodontitis induces microbiota-gut-brain axis disorders and cognitive impairment in mice, Exp. Neurol. 326 (2020) 113176.
[17] Y. Zhao, Y. Chen, X. Hu, et al., lncRNA LINC01535 upregulates BMP2 expression levels to promote osteogenic differentiation via sponging miR-3619-5p, Mol. Med. Rep. 22 (6) (2020) 5428–5435.
[18] S. Wang, G. Xiong, R. Ning, et al., LncRNA MEG3 promotes osteogenesis of hBMSCs by regulating miR-21-5p/SOD3 axis, Acta Biochim. Pol. 69 (1) (2022) 71–77.
[19] W. Zhang, L. Chen, J. Wu, et al., Long noncoding RNA TUG1 inhibits osteogenesis of bone marrow mesenchymal stem cells via Smad5 after irradiation, Theranostics 9 (8) (2019) 2198–2208.
[20] N. Zhang, X. Hu, S. He, et al., LncRNA MSC-AS1 promotes osteogenic differentiation and alleviates osteoporosis through sponging microRNA-140-5p to upregulate BMP2, Biochem. Biophys. Res. Commun. 519 (4) (2019) 790–796.
[21] Y. Xu, W. Qin, D. Guo, et al., LncRNA-TWIST1 promoted osteogenic differentiation both in PPDLSCs and in HPDLSCs by inhibiting TWIST1 expression, BioMed Res. Int. 2019 (2019) 8735952.
[22] H. Chen, L. Chen, An integrated analysis of the competing endogenous RNA network and co-expression network revealed seven hub long non-coding RNAs in osteoarthritis, Bone Joint Res 9 (3) (2020) 90–98.
[23] B. Jia, Z. Wang, X. Sun, et al., Long noncoding RNA LINC00707 sponges miR-370-3p to promote osteogenesis of human bone marrow-derived mesenchymal stem cells through upregulating WNT2B, Stem Cell Res. Ther. 10 (1) (2019) 67.
[24] D.W. Zhang, H.G. Wang, K.B. Zhang, et al., LncRNA XIST facilitates S1P-mediated osteoclast differentiation via interacting with FUS, J. Bone Miner. Metabol. 40 (2) (2022) 240–250.
[25] D.J. Li, G.Q. Liu, X.J. Xu, Silence of lncRNA BCAR4 alleviates the deterioration of osteoporosis, Eur. Rev. Med. Pharmacol. Sci. 24 (11) (2020) 5905–5913.

[26] Y. Li, M. Yan, Z. Wang, et al., 17beta-estradiol promotes the odonto/osteogenic differentiation of stem cells from apical papilla via mitogen-activated protein kinase pathway, Stem Cell Res. Ther. 5 (6) (2014) 125.
[27] Y. Wei, H. Ma, H. Zhou, et al., miR-424-5p shuttled by bone marrow stem cells-derived exosomes attenuates osteogenesis via regulating WIF1-mediated Wnt/β-catenin axis, Aging (Albany NY) 13 (13) (2021) 17190–17201.
[28] D. Wu, X. Chang, J. Tian, et al., Bone mesenchymal stem cells stimulation by magnetic nanoparticles and a static magnetic field: release of exosomal miR-1260a improves osteogenesis and angiogenesis, J. Nanobiotechnol. 19 (1) (2021) 209.
[29] Y.T. Sun, J.H. Cai, S. Bao, Overexpression of lncRNA HCP5 in human umbilical cord mesenchymal stem cell-derived exosomes promoted the proliferation and inhibited the apoptosis of ovarian granulosa cells via the musashi RNA-binding protein 2/oestrogen receptor alpha 1 axis, Endocr. J. 69 (9) (2022) 1117–1129.
[30] G. Miao, B. Liu, K. Ling, et al., Long noncoding RNA HCP5 contributes to nasopharyngeal carcinoma progression by targeting MicroRNA-128-3p, JAMA Oncol. 2022 (2022) 5740857.
[31] B. Yuan, Q. Guan, T. Yan, et al., LncRNA HCP5 regulates pancreatic cancer progression by miR-140-5p/CDK8 Axis, Cancer Biother. Radiopharm. 35 (9) (2020) 711–719.
[32] X. Li, B. Chen, A. Huang, et al., LncRNA HCP5 enhances the proliferation and migration of cervical cancer via miR-216a-5p/CDC42 axis, J. Cancer 13 (6) (2022) 1882–1894.
[33] W.K. Yun, Y.M. Hu, C.B. Zhao, et al., HCP5 promotes colon cancer development by activating AP1G1 via PI3K/AKT pathway, Eur. Rev. Med. Pharmacol. Sci. 23 (7) (2019) 2786–2793.
[34] M. Lei, Z. Jingjing, J. Tao, et al., LncRNA HCP5 promotes LAML progression via PSMB8-mediated PI3K/AKT pathway activation, Naunyn-Schmiedeberg's Arch. Pharmacol. 393 (6) (2020) 1025–1032.
[35] Y. Guo, L. Wang, H. Yang, et al., Knockdown long non-coding RNA HCP5 enhances the radiosensitivity of esophageal carcinoma by modulating AKT signaling activation, Bioengineered 13 (1) (2022) 884–893.
[36] S. Zhang, H. Huangfu, Q. Zhao, et al., Downregulation of long noncoding RNA HCP5/miR-216a-5p/ZEB1 axis inhibits the malignant biological function of laryngeal squamous cell carcinoma cells, Front. Immunol. 13 (2022) 1022677.
[37] X. Deng, F. Ye, L. Zeng, et al., Dexmedetomidine mitigates myocardial ischemia/reperfusion-induced mitochondrial apoptosis through targeting lncRNA HCP5, Am. J. Chin. Med. 50 (6) (2022) 1529–1551.
[38] J.D. Gao, R.J. Li, P.L. Ma, et al., Knockdown of lncRNA HCP5 protects against cerebral ischemia/reperfusion injury by regulating miR-652-3p, J. Biol. Regul. Homeost. Agents 34 (3) (2020) 893–900.
[39] M. Kong, H. Li, W. Yuan, et al., The role of Circ_PRKCI/miR-24-3p in the metastasis of prostate cancer, J buon 26 (3) (2021) 949–955.
[40] F. Wang, T. Gu, Y. Chen, et al., Long non-coding RNA SOX21-AS1 modulates lung cancer progress upon microRNA miR-24-3p/PIM2 axis, Bioengineered 12 (1) (2021) 6724–6737.
[41] X. Han, Q. Li, C. Liu, et al., Overexpression miR-24-3p repressed Bim expression to confer tamoxifen resistance in breast cancer, J. Cell. Biochem. 120 (8) (2019) 12966–12976.
[42] Y. Wu, K. Lian, C. Sun, LncRNA LEF1-AS1 promotes osteogenic differentiation of dental pulp stem cells via sponging miR-24-3p, Mol. Cell. Biochem. 475 (1–2) (2020) 161–169.
[43] X.S. Bai, P. Zhang, Y.S. Liu, et al., TRIB3 promotes osteogenic differentiation of human adipose-derived mesenchymal stem cells levelled by post-transcriptional regulation of miR-24-3p, Chin. J. Dent. Res. 24 (4) (2021) 235–249.
[44] M. Pang, H.X. Wei, X. Chen, Long non-coding RNA potassium voltage-gated channel subfamily Q member 1 overlapping transcript 1 regulates the proliferation and osteogenic differentiation of human periodontal ligament stem cells by targeting miR-24-3p, Hua xi kou qiang yi xue za zhi 39 (5) (2021) 547–554.
[45] N. Verheijen, C.M. Suttorp, R.E.M. Van Rheden, et al., CXCL12-CXCR4 interplay facilitates palatal osteogenesis in mice, Front. Cell Dev. Biol. 8 (2020) 771.
[46] L.F. Zhang, J. Qi, G. Zuo, et al., Osteoblast-secreted factors promote proliferation and osteogenic differentiation of bone marrow stromal cells via VEGF/heme-oxygenase-1 pathway, PLoS One 9 (6) (2014) e99946.
[47] A.R. Kim, Y.J. Lim, W.G. Jang, Zingerone stimulates osteoblast differentiation by increasing Smad1/5/9-mediated HO-1 expression in MC3T3-E1 cells and primary mouse calvarial cells, Clin. Exp. Pharmacol. Physiol. 49 (10) (2022) 1050–1058.
[48] A. Besnard, B. Galan-Rodriguez, P. Vanhoutte, et al., Elk-1 a transcription factor with multiple facets in the brain, Front. Neurosci. 5 (2011) 35.
[49] A.D. Sharrocks, The ETS-domain transcription factor family, Nat. Rev. Mol. Cell Biol. 2 (11) (2001) 827–837.
[50] J. Zou, C. Xu, Z.W. Zhao, et al., Asprosin inhibits macrophage lipid accumulation and reduces atherosclerotic burden by up-regulating ABCA1 and ABCG1 expression via the p38/Elk-1 pathway, J. Transl. Med. 20 (1) (2022) 337.
[51] Y. Deng, L. Li, J.H. Zhu, et al., COX-2 promotes the osteogenic potential of BMP9 through TGF-β1/p38 signaling in mesenchymal stem cells, Aging (Albany NY) 13 (8) (2021) 11336–11351.
[52] Y. Liu, L. Zeng, W. Wang, et al., [Human bone marrow mesenchymal stem cell exosome-derived miR-335-5p promotes osteogenic differentiation of human periodontal ligament stem cells to alleviate periodontitis by downregulating DKK1, Nan Fang Yi Ke Da Xue Xue Bao 43 (3) (2023) 420–427.